View metadata, citation and similar papers at core.ac.uk

brought to you by CORE

provided by Engineering Conferences International

Refereed Proceedings

The 12th International Conference on Fluidization - New Horizons in Fluidization Engineering

Engineering Conferences International *Year* 2007

Drying of Moist Solid Particulate in a Bubbling Fluidised Bed

Yassir Makkawi* Jamie Duncan†

Marc McAndrew‡ Raffaella Ocone**

*Heriot-Watt University

†Heriot-Watt University

‡Heriot-Watt University

**Heriot-Watt University, R.Ocone@hw.ac.uk

This paper is posted at ECI Digital Archives.

http://dc.engconfintl.org/fluidization_xii/27

DRYING OF MOIST SOLID PARTICULATE IN A BUBBLING FLUIDISED BED

Yassir Makkawi, Jamie Duncan, Marc McAndrew, Raffaella Ocone*
Chemical Engineering, School of Engineering and Physical Sciences, Heriot-Watt University, Edinburgh EH14 4AS, UK
* +44 (0) 131 451 3777; Fax: +44 (0) 131 451 3129; email: r.ocone@hw.ac.uk

ABSTRACT

Air at ambient conditions was used to dry moist particles at various fluidisation velocities. Throughout the drying process, images of the material distribution were recorded using Electrical Capacitance Tomography (ECT). Simultaneously, the outlet air moisture content was measured using temperature/humidity probe. The ECT data were used to quantify the bubbles characteristics while the air moisture content was used to calculate the drying rate. To avoid the complexity of the process, the fluidised bed was operated at single bubbling regime. The experimental results are discussed in relation to the different drying mechanisms.

INTRODUCTION

Bubbling fluidised beds are one of the most convenient means for interaction between solid and gas flow, mainly due to the good mixing and high heat and mass transfer rate. When applied to drying of non-porous wetted solid particles, the water is drawn-off the bed driven by the difference in water concentration between the bubble phase and the phases. This process may occur under different mechanisms depending on the bed hydrodynamics (i.e. bubbles characteristics) and the water content in the bed. Therefore, the design of bubbling fluidised bed dryer requires understanding of the combined complexity in hydrodynamics and mass transfer mechanism.

In gas-solid fluidised bed drying there are three different phases which all contribute in the draw-off moisture from wet particles. These are the bubble phase, its surrounding cloud phase and the dense annular phase. Adding to this, the drying process occurs in two stages: fast drying period, usually referred to by “constant drying rate regime” followed by slow drying rate, usually referred to as “falling drying rate regime”. Thus in experimental determination of the overall mass transfer coefficient, one must have in hand detailed quantitative data on the bubble characteristics as well as the drying rate.

In this study we measured the overall mass transfer coefficient in a conventional bubbling fluidised bed dryer. The drying rate and the corresponding mass balance

The 12th International Conference on Fluidization - New Horizons in Fluidization Engineering, Art. 27 [2007]

were calculated from the measured condition of the drying air at outlet. Information on the bed hydrodynamics was obtained from the imaging technique, Electrical Capacitance Tomography (ECT).

EXPERIMENTAL

The primary objective of the experiments was to measure the mass transfer coefficient for drying process in a conventional bubbling fluidised bed. This required detailed knowledge of the fluidised bed hydrodynamics and drying rate. For this purpose, wet solid particles were introduced in a vertical column and fluidised using air at ambient temperature. The fluidising air was virtually dry and obtained from a high-pressure compressor. An advanced imaging ECT sensor was used to provide dynamic information on the fluidised bed material distribution. The outlet temperature and the relative humidity of the fluidising air were recorded using a temperature/humidity probe.

Experimental Procedure

The experimental procedure employed here was completely non-intrusive. This is described in the following steps in the order of their occurrence:

(a) A total weight of 4.5 kg dry ballotini mixture was placed in a granule shaker after being wetted by distilled water. The shaker was firmly clamped and operated continuously for at least 20 minutes to ensure even distribution of water content.

(b) The wetted particles were then loaded into the fluidisation column. The ECT sensor was calibrated for the two extreme cases. This was carried out by sliding the ECT sensor up to the freeboard to calibrate for the empty bed case and down to the static bed area to calibrate for the packed bed case. Since the water content was limited to a maximum of 45 ml (1% moisture on dry solid weight basis) the possible changes in the particle/air permittivity during the drying process would be negligible.

(c) The wet bed material was fluidised at the required air flow rate. This was carefully adjusted to ensure the bed operation at the single bubble regime. The temperature and relative humidity were recorded at the intervals of 2 minutes. Simultaneously, and at the intervals of 5 minutes, a segment of 60 seconds ECT data was recorded. The expanded bed height during fluidisation was obtained from visual observations.

(d) The drying rate was obtained from the measured air flow rate and temperature/humidity data at inlet and outlet using psychometric charts and mass balance calculations. The recorded ECT data was further processed off-line and loaded into in-house developed MATLAB software to estimate the bubble characteristics.

The above described procedure was repeated for the three different operating conditions summarised in Table 1.

Measurement of mass transfer coefficient

Considering a section of the bed as shown in Fig. 1, the overall mass transfer coefficient between the bubble phase and the surrounding dense phase, k_{db}, can be defined by the following rate equation:

$$-u_b \frac{dC_b}{dz} = \left(\frac{S_b}{V_b}\right) k_{db}(C_d - C_b) \quad (1)$$

where C_b is the water concentration in the bubble phase, C_d is the concentration in the surrounding dense phase, u_b, S_b and V_b are characteristic features of the bubble representing the rising velocity, interphase area and volume, respectively. For moisture-free inlet air, Eq. 1 is subject to the following boundary conditions:

$$C_b = (C_{in})_{air} = 0 \text{ at } z = 0 \quad \text{and} \quad C_b = (C_{out})_b \text{ at } z = H \quad (2)$$

Because the bubbles rise much faster than the gas velocity thought the dense phase, the contribution of the gas flow through the dense phase is assumed negligible. Thus, the bubble moisture content at the outlet $(C_{out})_b$ is given by:

$$(C_{out})_b = \frac{\text{(drying rate)}}{\text{(bubble mass flow rate)}} = \frac{m_{air}(C_{out} - C_{in})_{air}}{m_b} \quad (3)$$

where m_{air} is the mass flow rate of the fluidising air and $(C_{out})_{air}$ is the water concentration at air outlet, obtained indirectly from the measured temperature and humidity at the bubbling bed surface. Since the inlet air was virtually dry, $(C_{in})_{air}$ is taken as zero and Eq. 3 reduces to:

$$(C_{out})_b = m_{air}(C_{out})_{air} / m_b \quad (4)$$

For a spherical bubble, the ratio S_b/V_b appearing in Eq. 1 reduces to $6/d_b$, where d_b is the bubble diameter. For a perforated distributor (such as the one used in this experiment), bubbles coalescence mainly at a few centimetres above the distributor, therefore, the entrance effect is neglected and the bubble characteristics are assumed independent of the height (this was confirmed from the ECT images).

Finally, assuming that the water concentration in the dense phase is uniform and remains unchanged during the bubble rise ($C_d = w_{water}/w_{bed}$), integration of Eq. 1 from $z = 0$ to $z = H$ gives the mass transfer coefficient as follows:

$$k_{db} = -\left(\frac{d_b u_b}{6H}\right) \ln\left[\frac{C_d - (C_{out})_b}{C_d}\right] \quad (5)$$

where d_b, u_b and H are the bubble diameter, bubble velocity and the expanded bed height respectively.

Measurement of bubble characteristics

Experimental determination of the overall mass transfer requires knowledge of the bubble diameter and velocity (see Eq. 5). The ECT is capable of determining the size and velocity of bubbles or 'voids' in a gas-solid fluidised bed. The distinct lowering of the solid fraction at the moment of bubble passage across the sensor area allows identification of the bubble events in a given time and space. The bubble velocity was then calculated from the delay time determined from detailed analysis of the signal produced by the two adjacent sensors, such that:

$$u_b = \delta/(\Delta t_b) \quad (6)$$

where $\Delta t_b = t_{b2} - t_{b1}$, t_{b1} and t_{b2} represent the time when the bubble peak passes through the lower and upper level sensors respectively, and δ represents the distance between the centre of the two sensors, which is 3.8 cm. The method is demonstrated in a typical ECT data in Fig. 2.

The bubble diameter was obtained from the ECT data of relative solid fraction at the moment of bubble peak across the sensor cross-section. From this, the bubble voidage fraction (the fraction of the bed occupied by bubbles) is calculated as follows:

$$\delta_b = (1 - P) \tag{7}$$

$$d_b = D(1 - P) \tag{8}$$

where δ_b is the bubble fraction and P is the relative solid fraction (i.e. packed bed: $P = 1$; empty bed: $P = 0$) and D is the bed/column diameter. This procedure is demonstrated in a typical ECT data in Fig. 2.

With the bubble velocity and bubble fraction in hand, the bubble mass flow rate was calculated as follows:

$$m_b = \delta_b u_b A \rho_{air} \tag{9}$$

Further details on the application of twin-plane ECT in the measurements of bubble characteristics in fluidised bed can be found in Makkawi and Wright (2004).

RESULTS AND DISCUSSION

Hydrodynamics

Fig. 3 shows the measured bubble velocity and bubble diameter as function of the water content in the bed. These measurements were taken at different time intervals during the drying process. Each data point represents the average over a segment of 60 seconds. Both parameters seem to vary slightly within a limited range. These hydrodynamic observations suggest that that the bubble characteristics almost remain independent of the water content, at least within the range of operation conditions considered here. This is due to the fact that the initial water content in the bed was not large enough to cause considerable hydrodynamic changes.

Among the many available correlations, the following equations have been found to provide the best match with the experimental measurements:

Bubble velocity (Davidson and Harrison, 1963):

$$U_b = \psi(U - U_{mf}) + \alpha\left[0.711(g d_b)^{0.5}\right] \tag{19}$$

where $\psi = 0.75$ and $\alpha = 3.2 D_c^{1/3}$ are correction factors suggested by Werther (1978) and Hilligardt and Werther (1986).

Bubble diameter (Mori and Wen, 1975):

$$d_b = 0.652\left[D_o - \exp(-0.3\, z/D_c)\right] + \frac{0.347 D_o}{n_o^{0.4}} \exp(-0.3\, z/D_c) \tag{20}$$

where

$$D_o = \left[\frac{\pi}{4D_c^2} \left(U - U_{mf} \right) \right]^{0.4} \quad (21)$$

The predicted U_{mf} used in the theoretical estimation of U_b and d_b was given by (Kunii and Levenspiel, 1991):

$$U_{mf} = \frac{d_p^2 \left(\rho_p - \rho_g \right) g}{150 \mu} \frac{\varepsilon_{mf}^3 \phi_p}{\left(1 - \varepsilon_{mf} \right)} \quad (22)$$

This gives U_{mf} =0.065 m/s, which closely matches the experimental value of 0.062 m/s. Despite the fact that Eqs.19-22 were originally developed for dry bed operation, they seem to provide reasonable match with the experimental measurement. This is not surprising because the water content in the bed was relatively low as discussed above. The expanded bed height, used in the experimental estimation of the overall mass transfer coefficient (Eq. 5), is shown in Fig. 4. A gradual but limited increase in the bed expansion, as the water is drawn off the bed, can be noticed.

Drying rate

The drying rate curves for the three conducted experiments are shown in Fig. 5. The polynomial curve fitting describes the water content in the bed at various times. From this figure there is strong evidence that the drying mechanism occurs in two different rates, first fast drying period followed by a slow drying period eventually leading to the end of the process. The results also demonstrated that the time needed to reach the slow drying rate is directly proportional to the initial water content and inversely proportional to the drying air flow rate. For instance, at an air velocity of 0.47 m/s, this time was reduced by half when reducing the initial water content from $C_{o,bed}$ =10 to $C_{o,bed}$ =5%, while at the initial water content of $C_{o,bed}$ =10, this time was ~35% longer when reducing the air velocity from 0.47 m/s to 0.33 m/s.

The water concentration in the bed (g/kg dry solid) as function of the drying time is shown in Fig. 6. The water content at any time during the drying process was obtained from the integration of the drying curve function, $F(t)$, and subtracting from the initial water content, w_o, such that:

$$w_t = w_o - \int_0^t F(t) dt \quad (23)$$

In Fig. 6, it is clear that commence of the slow drying period for the three curves coincides at the critical water concentration of C_{bed} =2.

Experimental measurement of mass transfer

Fig. 7 shows the experimentally measure overall mass transfer coefficient, k_{db}, as function of time for one selected experiment. The mass transfer coefficient at the fast drying rate period is massively higher than the coefficients measured at the slow drying rate period. The coefficients at the first rate ideally seems to fall in a straight line, while at the slow rate the values sharply drop to a low value and slowly decreases towards zero as the solid surface approaches equilibrium with the drying air. This difference is mainly attributed to the difference in the drying mechanism.

Published by ECI Digital Archives, 2007

The 12th International Conference on Fluidization – New Horizons in Fluidization Engineering, Art. 27 [2007]

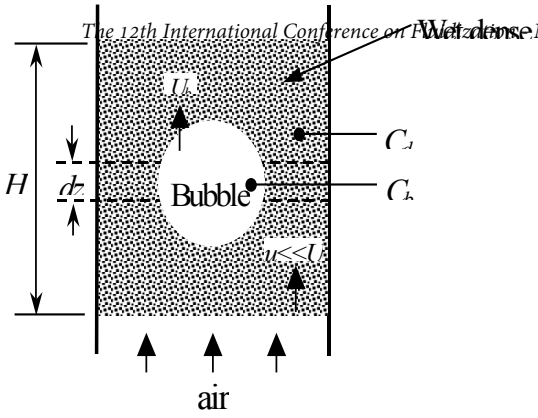

Fig.1. Schematic representation of the method used in experimental calculation of the overall mass transfer coefficient.

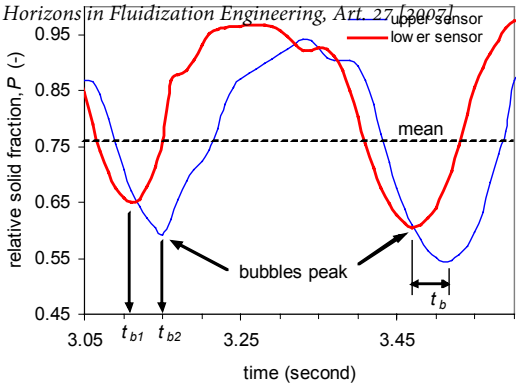

Fig. 2 Estimation of bubble velocity from ECT data.

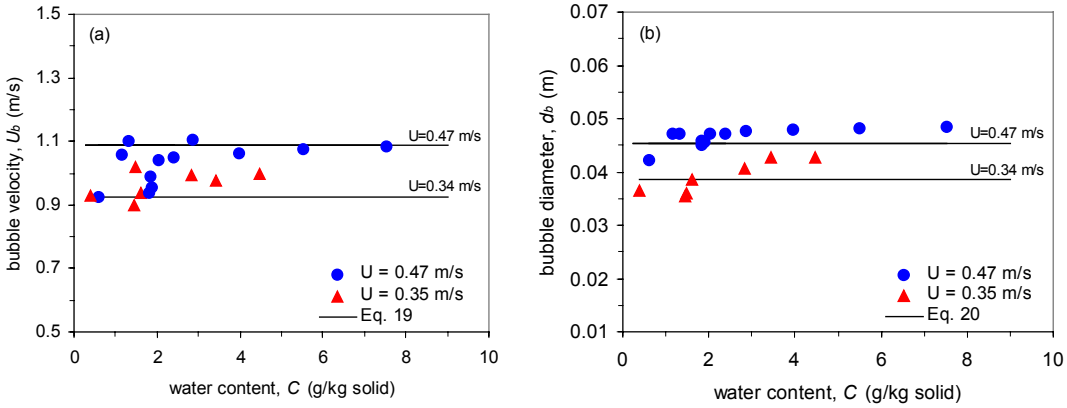

Fig. 3 Variation of the bubble velocity and bubble diameter during the drying process.

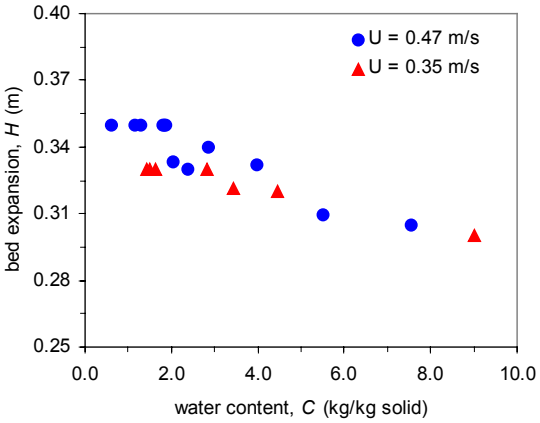

Fig. 4 Variation of the expanded fluidised bed height.

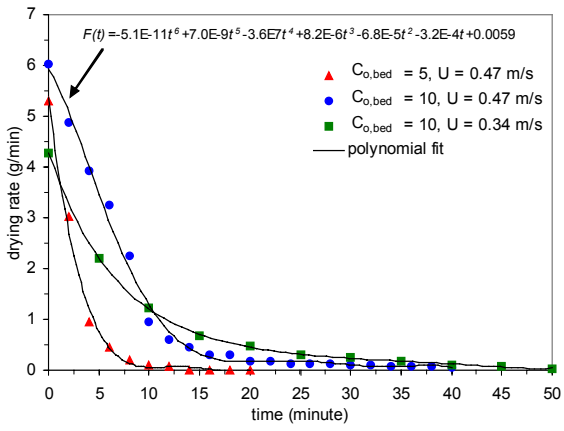

Fig 5 Drying rate curves for three experiments during the drying process

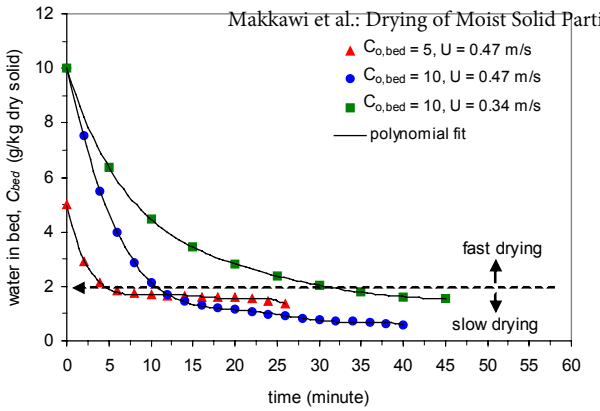

Fig. 6 Variation of water content during drying

At high water content, the migration of the free water from the particle surface is faster due to the high driving force, then beyond the critical water concentration, at C=2, the thin water layer surrounding the particle, is physically bonded with the particles surface due to surface tension, this considerably hinders the drying process. This behaviour should not be confused with the case of porous particles were such phenomena occur as a result of the water molecules being trapped between the particles pores, thus experiencing considerable internal diffusion resistance before reaching the particle surface.

The measured overall mass transfer coefficient for the three conducted experiments as function of the water concentration in the bed is shown in Fig. 8. At the fast drying rate period, the values of k_{db} falls within the range of 0.0145-0.021 m/s. It is interesting to note that this range is close to literature value for the mass transfer coefficient from a free water surface to an adjacent slow moving ambient air stream (~0.015 m/s). At the slow drying rate period, k_{db} is very low and falls within the range of 0.0002-0.0037 m/s.

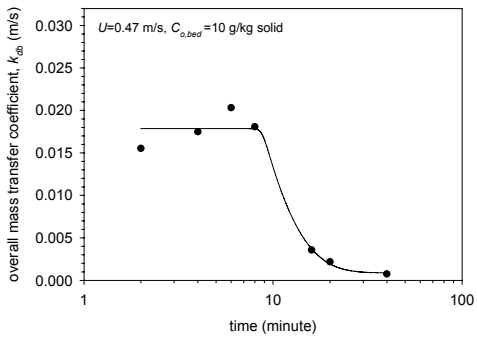

Fig. 7 Experimentally measured overall mass transfer coefficient for one selected experiment.

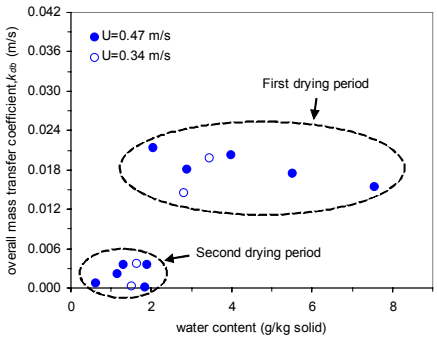

Fig. 8 Mass transfer coefficient measured at two drying periods.

CONCLUSIONS

Mass transfer coefficient in a bubbling fluidised bed dryer has been experimentally determined. This work is the first to utilise the ECT system for this purpose. The ECT

The 12th International Conference on Fluidization - New Horizons in Fluidization Engineering, Art. 27 [2007]

allowed estimation of the bubble diameter and velocity as well as observation on bubble-cloud-dense boundaries.

In the first drying period, defined at the critical water concentration $C > 2$, the overall mass transfer coefficient was relatively constant, varying within a limited range of 0.045-0.021 m^2/s. In this range, the boundaries for the overall mass transfer coefficient are best represent by: (i) model accounting for diffusional resistance as well as the bubble throughflow, giving the lower limit (Eq. 16) and (ii) model accounting for the diffusional resistance at the cloud-bubble interface, giving the upper limit (Eq. 12).

In the second drying period, the drying efficiency was considerably low and gradually decreases towards zero as the bed material approaches equilibrium with the humidity of drying air. The measured overall mass transfer coefficient was in the range of 0.0002-0.0037 m^2/s. Because the particles used were non-porous glass beads, this behaviour is presumably due to the increased effect of particle surface tension. In this range, the contribution of cloud-bubble interchange is overestimated and should be neglected.

This work emphasises the importance of further experimental study. In order to obtain a generalised correlation for the mass transfer coefficient, it is highly recommended that a comprehensive experimental program should be considered covering a wider range of operating conditions (particle size, gas velocity, water content, porous/non-porous particles). Such a correlation is of vital importance for improved fluidised bed dryer design and operation.

Table 1 Summary of experimental runs

Exp. No.	Bed loading (kg)	Fluidization velocity (m/s)	Initial water content wt% (dry basis)
1	4.5	0.34	1.0
2	4.5	0.47	1.0
3	4.5	0.47	0.5

ACKNOWLEDGEMENT: The authors thank the UK's Engineering and Physical Science Research Council (*EPSRC*) for a research grant (Ref. *GR/R85778*).

REFERENCES

1. Davidson, J., Harrison, D., Fluidized Particles, Cambridge University Press, Cambridge, UK (1963)
2. Hilligardt, K., and Werther, J., German Chemical Engineering 9 (1986) 215. In Kunii, D., and Levenspiel, O., Fluidization Engineering. Second edition, Butterworth-Heinemann, Boston (1991)
3. Kunii, D., and Levenspiel, O., Fluidization Engineering. Second edition, Butterworth-Heinemann, Boston (1991)
4. Makkawi, Y. and Wright, P. C., Powder Technology 148 (2004) 142-157.
5. Mori, S., Wen, C. Y., AICHE J. 21 (1975) 109-115
6. Werher, J. German Chemical Engineering 1 (1978) 166. In Kunii, D., and Levenspiel, O., Fluidization Engineering. Second edition, Butterworth-Heinemann, Boston (1991)